J. Braz. Chem. Soc., Vol. 24, No. 1, 40-50, 2013.
Printed in Brazil - ©2013 Sociedade Brasileira de Química
0103 - 5053 $6.00+0.00

Article

Characterization of ZSM-5 Modified with Niobium Pentoxide: the Study of Thiophene Adsorption

Rodrigo M. Cavalcanti,[a] Ivoneide de C. L. Barros,[a] José A. Dias[b] and Sílvia C. L. Dias[b]*

[a]*Instituto de Ciências Exatas, Universidade Federal do Amazonas, Av. Gen. Rodrigo Otávio Jordão Ramos, 6200, 69077-000 Manaus-AM, Brazil*

[b]*Instituto de Química, Campus Darcy Ribeiro, Universidade de Brasília, CP 4478, 70904-970 Brasília-DF, Brazil*

Adsorventes ZSM-5 impregnados com Nb_2O_5 foram aplicados na remoção de enxofre sob a forma de tiofeno, substância refratária de difícil remoção dos combustíveis líquidos. Para tanto, foi preparado um combustível modelo contendo iso-octano contaminado com tiofeno nas concentrações de 877,5 a 1155 ppmw. As amostras foram caracterizadas por difratometria de raios X (XRD), espectroscopias no infravermelho (FTIR) e Raman (FT-Raman) por transformada de Fourier para confirmação dos adsorventes obtidos, sendo priorizado o estudo de adsorção com aquele contendo 5% de pentóxido de nióbio, que apresentou uma maior capacidade de remoção de tiofeno. Os melhores resultados de adsorção foram alcançados a 353 K, sendo observado um maior tempo para atingir o equilíbrio. Sob essas condições, o melhor ajuste cinético foi alcançado utilizando a equação de pseudo-segunda ordem, evidenciando o domínio do fenômeno de quimissorção. Por outro lado, sob menores temperaturas, o modelo de difusão apresentou uma melhor aproximação dos resultados experimentais. O aumento da temperatura também favoreceu os processos espontâneos.

ZSM-5 adsorbents impregnated with Nb_2O_5 were applied in the sulfur removal in the form of thiophene, refractory substance of difficult removal of liquid fuels. For this purpose, a model fuel containing iso-octane contaminated with thiophene in concentrations of 877.5 to 1155 ppmw was prepared. The samples were characterized by X-ray diffractometry (XRD), Fourier transform infrared (FTIR) and Fourier transform-Raman (FT-Raman) spectroscopies for confirmation of the adsorbents, being prioritized the adsorption study with that containing 5 wt.% of niobium pentoxide, because it showed a greater capacity for removal of thiophene. The best results of adsorption were achieved at 353 K, a longer time to reach equilibrium was observed. Under these conditions, the best kinetic fitting was achieved using the equation of pseudo-second order, demonstrating the domain of the phenomenon of chemisorption. While under lower temperatures, the diffusion model presented a better approximation of the experimental results. Also, the increasing of temperature did enhance spontaneous processes.

Keywords: ZSM-5 zeolite, niobium pentoxide, kinetics, adsorption, thiophene

Introduction

The removal of sulfur (S) from fossil fuels has been stimulated for some years by the implementation of legislation that restricts the amount of S to values lower than 100 ppmw.[1] Petroleum contains approximately 0.06-8.00% m/m of sulfur, with the higher concentrations in heavier fractions of crude oil.[2] Gasoline obtained by cracking, for example, is responsible for most of sulfur content in commercial gasoline.[3] Combustion of these fuels in internal combustion engines emits SO_x. Even at lower concentrations, SO_x can poison catalysts designed for exhaust gas treatment.[4] In 1993, a dramatic reduction in S concentration from 5000 to 500 ppmw was promoted. In 2006, the proposed goal was 30 ppmw for gasoline and 15 ppmw for diesel.[5,6]

The decrease in S content represents a huge technological demand because the sulfur present in fuel is not in its elemental form, but exists as a heteroatom in organosulfur compounds. These species include mercaptans (sulfides and RSH), disulfides (RSSR') and aromatics such as thiophene (T), dibenzothiophene (DBT) and related compounds.[7] The removal of these compounds should be

*e-mail: ibarros@ufam.edu.br

achievable via catalytic hydrodesulfurization processes (HDS). Derivatives of thiophene, however, are extremely refractory in conventional HDS processes.[8] Moreover, HDS requires significant investments for refineries for both installation and maintenance due to the high temperatures and pressures and sophisticated catalysts required for its operation. The new restrictions would force the building of facilities for HDS that are 5 to 15 times larger than those existing, and the conditions required for these processes would be much more severe, leading to a reduced lifetime for the catalysts.[1,9]

An alternative process for reduction of the sulfur compounds in fuels that generates less environmentally hazardous products at a lower cost than that of HDS is adsorption, especially for thiophene. Materials such as zeolites and coals have already been employed based on the principle that these adsorbents are capable of selectively capturing organosulfur compounds such as thiols (mercaptans) and thiophene and its derivatives. One example is the study of adsorbents based on Y zeolite modified with transition metals (Cu, Ni, Zn, Pd and Ce) for use in the desulfurization of aviation fuels.[4] Zeolites Y and Beta have also been modified with Zn for the adsorption of benzothiophene and dibenzothiophene contaminants in cyclohexane-based model fuels.[10] Studies employing Ag^+-exchanged mesopourous Al-MSU-S showed very promising results for the adsorption of thiophene and benzothiophene in *n*-octane.[11] Research on copper Y zeolite has suggested that the interaction with thiophene compounds occurs selectively via π-complexation.[1,12-14]

In this study, ZSM-5 zeolite was chosen as adsorbent support due to its distribution of acid sites and pore geometry, which offer easy access and selectivity for molecules of thiophene.[15,16] Furthermore, niobium incorporated into these materials can display special properties that are not found in other transition metal composites. These properties, such as stability and strong interactions with the metal support, are extremely important for determining the quality of the adsorbent.[17] To evaluate the properties of the new adsorbent materials and to be able to predict the behavior of these solids in adsorption processes, the kinetics of the adsorption reaction of a model fuel containing *iso*-octane and *n*-octane were elucidated. This information was then used to determine key parameters of the adsorbent, such as the amount of sulfur contaminants adsorbed from the liquid fuel and the rate constant. The principal phenomena considered during the study of the adsorption kinetics were diffusion of molecules within the fluid phase to the interfacial region, diffusion of molecules inside the pores, diffusion of molecules on the surface and the elementary process of adsorption-desorption.[18]

Experimental

Materials

To prepare the adsorbent materials, $NH_4[NbO(C_2O_4)_2(H_2O)_2](H_2O)_n$, supplied by Companhia Brasileira de Metalurgia e Mineração (CBMM), and the ZSM-5 zeolite (Si/Al: 40, Na_2O: 0.5 wt.%) donated by Petrobras were used. The model fuels were prepared from *iso*-octane (Dinâmica, UV/HPLC grade), *n*-octane (Sigma-Aldrich, 98%) and thiophene (Sigma-Aldrich, ≥ 99%).

The adsorbent system Nb_2O_5/ZSM-5 (Nb(x)ZSM-5)

The adsorbents were prepared by aqueous impregnation method.[19] To a solid mixture of NH_4ZSM-5 and the ammonium oxalate complex of niobium containing a calculated concentration of Nb_2O_5 between 2-25 wt.%, it was added distilled water at a ratio of 10 mL g^{-1}. The mixture was stirred and heated at 80 °C until the water completely evaporated, and then it was cooled to room temperature. Calcination was achieved using a muffle furnace with a static air atmosphere. The sample was heated at 10 K min^{-1} up to 823 K and then held at that temperature for 2 h. In the activation phase, the adsorbent was heated at 10 K min^{-1} to 573 K and then held at that temperature for 4 h.

Characterization of the adsorbents

Powder X-ray diffraction (XRD) patterns were obtained using a Shimadzu XRD-6000 instrument with the K_α line of copper [Cu(K_α)] (30 kV and 30 mA). Each acquisition was made in the range 2θ / 5°-50° at a scan rate of 2° min^{-1}. Scanning electron microscopy (SEM) images of the samples were acquired using a FEI Quanta-250 scanning electron microscope. The acquisition was made at an acceleration voltage of 25 kV and the samples were dried and coated with gold before the analysis.

Infrared (IR) spectra were collected using a spectrometer Spectrum 2000 instrument (Perkin Elmer). The resolution applied to the spectra was 4 cm^{-1} with 256 scans. The samples were mixed with KBr (Merck) at a ratio of 1:100, dried and pelletized.

The textural characterization of the adsorbent material was obtained using an ASAP 2020 Physisorption Analyzer from Micromeritics. The nitrogen adsorption at 77 K was obtained from ca. 0.350 g samples pretreated by degassing at 473 K for 4 h after heating at a rate of 10 K min^{-1}.

Procedure for adsorption of thiophene

The sulfur adsorption reactions were conducted under reflux at temperatures ranging from 293-353 K for 10 to 360 min, while maintaining a 10 g L^{-1} dose of adsorbent. The model fuels were comprised of solutions of *n*-octane and *iso*-octane contaminated with thiophene in concentrations of 808.5 mg L^{-1} (1155 ppmw) and 605.5 mg L^{-1} (877.5 ppmw). The amount of sulfur remaining in the solution after the reaction was analyzed by X-ray fluorescence spectroscopy using a RayNy EDX-700 (Shimadzu) in the liquid mode in air at a voltage of 15 kV and a scan time of 100 min. The analyses were completed in the Laboratório de Pesquisa e Ensaios em Combustíveis (LAPEC) at the Instituto de Ciências Exatas (ICE), Universidade Federal do Amazonas (UFAM).

To calculate the amount of sulfur adsorbed on the solid phase, the following equation was used:

$$q_t = \frac{V \times (C_0 - C_t)}{W} \quad (1)$$

where C_0 is the initial concentration of S (mg L^{-1}), C_t is the concentration of S at time t (mg L^{-1}), V is the volume of the model fuel (L) and W is the mass of the adsorbent (g).

Kinetic study of adsorption

The kinetic models utilized in this work describe the solid-liquid interactions based on chemisorption and physisorption phenomena.[20-24]

Processes controlled by chemisorption

Pseudo-first order equation (PFOE)

The kinetics of adsorption in aqueous solutions was extensively examined using a pseudo-first order model, represented here by equation 2.

$$\frac{dq_t}{dt} = K_1 \times (q_e - q_t) \quad (2)$$

Its linear form can be defined as the following:

$$\log(q_e - q_t) = \log(q_e) - \left(\frac{K_1}{2.303}\right) \quad (3)$$

where K_1 is the rate constant of the pseudo-first order reaction (min^{-1}) and q_e is the adsorbed amount at equilibrium (mg g^{-1}).

Pseudo-second order equation (PSOE)

PSOE is applied in situations in which chemisorption of the adsorbate in the adsorbent suggests a more complex interaction with respect to the equilibrium between the adsorbate in solution and that adsorbed on the solid phase, as expressed by equation 4.

$$\frac{dq_t}{dt} = K_2 \times (q_e - q_t)^2 \quad (4)$$

The linear form of this equation is the following:

$$\frac{t}{q_t} = \left(\frac{1}{K_2 \times q_e^2}\right) + \left(\frac{t}{q_e}\right) \quad (5)$$

where K_2 is the kinetic constant of the reaction (g mg^{-1} min^{-1}).

Elovich's equation

The Elovich's model is used for the evaluation of the kinetics of the chemisorption of gases on solids, but can also be considered in this case. In the work of Ranjan *et al.*,[24] this model was used to describe the adsorption of arsenic contaminants in aqueous solutions. Equation 6 represents the Elovich's model.

$$\frac{dq_t}{dt} = a \times \exp(-b \times q_t) \quad (6)$$

where a is the rate of chemisorption at the initial instant (mg g^{-1} min^{-1}) and b is the length of the surface coverage for this process (g mg^{-1}), which is related to the activation energy.

For the linear form of this equation given the boundary conditions t = 0 to t = t, q_t = 0 to $q_t = q_t$, we have the following:

$$q_t = \left[\frac{\ln(a \times b)}{b}\right] + \frac{1}{b} \times \ln\left[t + \left(\frac{1}{a \times b}\right)\right] \quad (7)$$

for high values of *t* ($t \gg 1/(a\ b)$).

Processes controlled by diffusion and physisorption

Study of intra-particle diffusion

The effects of diffusive mass transfer can also be considered in batch adsorption processes under strong agitation and can be investigated using the mathematical model for intra-particle diffusion, as represented by equation 8.[25]

$$q_t = f \times t^{1/2} + C \quad (8)$$

where f is the coefficient of intra-particle diffusion (mg g^{-1} $min^{-0.5}$) and C (mg g^{-1}) is related to the fluid film thickness that surrounds the surface of the solid.

Bangham's equation

Bangham's model (equation 9) is used when the diffusion phenomena inside the pores are considered as a limiting step of the adsorption process because the physical interaction, rapid at first, slows down in the latter stages of the process.[22,25-27] The equation is shown below.

$$\log\left\{\log\left[\frac{C_0}{(C_0 - q_t \times m)}\right]\right\} = \log\left(\frac{K_0 \times m}{2.303 \times V}\right) + \alpha \times \log(t) \quad (9)$$

where α (< 1) and K_0 are constants.

The fit of the models was evaluated from the linear graphs obtained for each particular equation: pseudo-first order model [$\log(q_e - q_t)$ *vs.* t]; pseudo-second order [t/q_t *vs.* t]; Elovich's equation [q_t *vs.* ln t]; intra-particle diffusion [q_t *vs.* $t^{1/2}$]; and Bangham's equation [$\log[\log(C_0/(C_0 - q_t\, m))]$ *vs.* log t].[20,21]

Estimation of the thermodynamic parameters of adsorption

The thermodynamic parameters of adsorption, such as the Gibbs free energy of adsorption ($\Delta G°$), the heat of adsorption or enthalpy ($\Delta H°$) and the standard entropy change ($\Delta S°$) of adsorption were studied at a range of 301-353 K using the equations below (equations 10-12).[24]

$$K_t = \frac{C_{Ae}}{C_e} \quad (10)$$

$$\Delta G^o = -R \times T \times \ln(K_t) \quad (11)$$

$$\Delta G^o = \Delta H^o - T \times \Delta S^o \quad (12)$$

where C_{Ae} is the concentration of the adsorbate in the solid phase (mg L^{-1}), C_e is the concentration of the adsorbate in the solution (mg L^{-1}), at equilibrium. The T is the absolute temperature (K) and R is the universal gas constant (8.314 J mol^{-1} K^{-1}).

Results and Discussion

Characterization of the adsorbents

The preparation and characterization of the materials have been previously reported.[28] XRD (Figure S1 in the Supplementary Information (SI) section), IR and Raman (not shown) spectroscopic analyses were thus used to confirm the prepared materials.

XRD results indicated that no qualitative change in the crystalline structure of the ZSM-5 after impregnation with Nb_2O_5 was observed before and after calcination at 823 K. The three strongest peaks in the 2θ / 22.5-25.0° region were nearly coincidental in all of the XRD patterns, confirming the reflections characteristic of crystalline ZSM-5. According to the literature,[28] crystalline phase of Nb_2O_5 (hexagonal phase, TT) supported on silica-alumina was observed only above 10 wt.% of Nb_2O_5 at 1073 K.

Adsorption/desorption isotherms of N_2 for Nb(5)ZSM-5 (Figure S2 in the SI section) showed on the initial part (partial pressure, P/P_0 between 0.001 and 0.5) the presence of a pseudo-plateau of type I. This behavior is due to the presence of micropores with a diameter close to the size of the molecule to be adsorbed. An increase in the adsorbed amount at pressures very close to unity can be related both to the capillary condensation that occurs in pores of larger diameters and the phenomenon of interparticle capillary condensation.[29-34] According to Šolcová *et al.*,[35] the presence of poorly defined structural materials (such as carbonous materials) in ZSM-5 provides the appearance of larger-sized pores and, consequently, an increase in the slope of the final part of the isotherm was observed for the Nb(5)ZSM-5 system. The hysteresis at the end of the isotherm can be classified as a type H4, and is usually observed in type I adsorbents. The same isotherm profile can also be observed for the sample after adsorption of thiophene.

Because the prepared material is essentially microporous, the Langmuir model, which is most suitable for type I isotherms, was used to calculate the apparent surface area in the initial region of the isotherm ($0.01 \leq P/P_0 \leq 0.5$). The BET model (Brunauer, Emmett and Teller) was used for a simple comparison in a more restricted range of partial pressure ($0.05 \leq P/P_0 \leq 0.14$), following the recommendations of Sing *et al.*.[36]

Comparing the apparent surface area by BET (S_{BET}, m^2 g^{-1}) before and after calcination of the fresh zeolite ZSM-5, it showed a loss of 11%, which is associated with residual materials present in the solid before calcination. For the ZSM-5 with niobium, after calcination, an increase of about 34% on the apparent micropore area and equivalent micropore volume (Table 1) was observed. A decrease of 20% on external surface area after calcination was assigned to oxalate and ammonium decomposition and water.

From the analysis of the pore-size distribution (PSD), shown in Figure 1 (in combination with the data in Table 1), two important points were noted: (*i*) calcining the adsorbent resulted in an appearance of smaller pore radius (0.23 nm) and an increase of 32% in the surface area; (*ii*) after adsorption of thiophene, a decrease of 8 and 11% on micropore area and volume was observed, respectively. The possible explanation for the point (*i*) is that the deposition of the niobium oxide occurred both in the external surface and in the entrance of the pores of the zeolite, if taken into account the dimensions of the

Table 1. Surface parameters of the adsorbent system Nb(5)ZSM-5

Sample	Apparent surface area / (m^2 g^{-1})				Equivalent volume / (cm^3 g^{-1})
	BET	Langmuir	Micropore (*t*-plot)	External surface (*t*-plot)	Micropore (*t*-plot)
ZSM-5 not calcined	356.7	–	–	–	–
ZSM-5 calcined	318.8				
Nb(5)ZSM-5 not calcined	279.4	325.7	318.8	6.9	0.11
Nb(5)ZSM-5 calcined	362.1	431.5	426.0	5.5	0.15
Nb(5)ZSM-5 after adsorption	305.5	401.3	390.3	11.0	0.13

ammonium niobium oxalate.[37] Thus, when the adsorbent was calcined, the removal of oxalate and ammonium allowed access to the pores of ZSM-5, however, the niobium oxide in the surroundings partially reduced their size, when compared to the pure ZSM-5.[38] After adsorption (*ii*), probably the channels became partial blocked by thiophene.

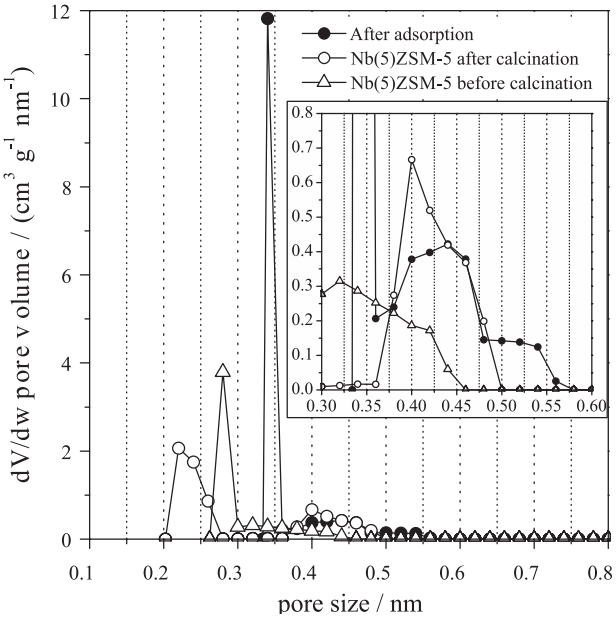

Figure 1. Pore size distribution (PSD) of the Nb(5)ZSM-5 adsorbent system.

According to the images obtained by scanning electron microscopy (SEM), the samples of Nb(5)ZSM-5 have a wide particle size ranging from 5-500 μm (Figure 2), and the larger particles (Figures 2b and 2d) are in fact clusters of smaller particles, as seen in Figure 2c. These larger sizes corroborate the N_2 isotherm adsorption results and the phenomena encountered in the study of the adsorption kinetics discussed below. Compared with the results of Bi *et al.*,[39] the zeolite modified with Nb maintained a microscale size in the range of 1-5 μm. There are, however, large clusters of up to 100 times that size.

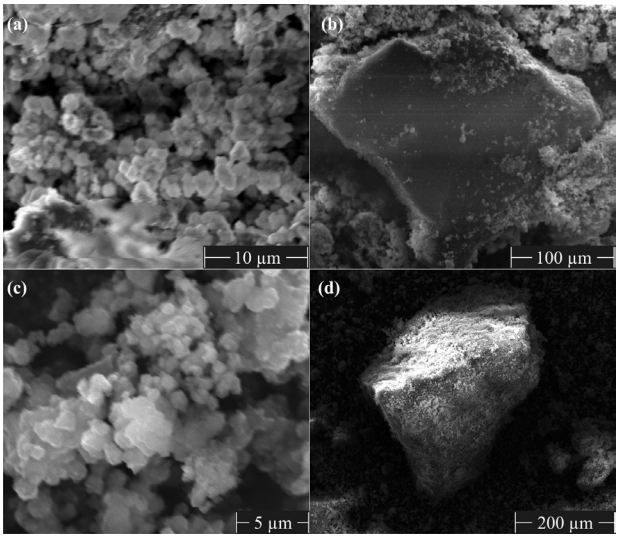

Figure 2. SEM images in different magnifications at 25 kV of Nb(5)ZSM-5 before (a) and (b) and after calcination at 823 K for 2 h (c) and (d).

Effect of Nb_2O_5 on the adsorption

Considering the studied adsorbents, Nb(x)ZSM-5 (x = 0, 2, 5, 10, 15% Nb_2O_5), Nb(5)ZSM-5 gave the best performance for sulfur removal of model fuel, with the amount of 43.58 mg g^{-1} of S.

In all tests, the modified zeolites, Nb(x)ZSM-5 achieved a level of S adsorption greater than that of the pure zeolite (24.21 mg g^{-1} of S). The initial removal, with 2% Nb_2O_5 (Nb(2)ZSM-5), approached 46.5% S, while the zeolites impregnated with 5-15% of Nb_2O_5 showed better adsorption capacities. This reinforces the evidence that the presence of the oxide on the zeolite plays an important role in the removal of sulfur in an organic medium. The lower level of adsorption displayed for Nb(2)ZSM-5 can be explained by the lower content of Nb, suggesting that the thiophene seems to be dependent on the load of Nb present in the zeolite.

At an impregnation level greater than 15% of Nb_2O_5, the efficiency of the solid starts to decrease (Table 2)

Table 2. Chemical analysis by XRF of the sulfur concentration in solution after adsorption at 353 K for 4 h

Sample	XRF of S (by mass)		
	Solution 1 (C_0 = 808.50 mg L^{-1} S)		
	S content in solution / (mg L^{-1})	Removal[a] of S / %	Amount adsorbed / (mg g^{-1})
ZSM-5	566.37	29.9	24.21
Nb(2)ZSM-5	432.81	46.5	37.57
Nb(5)ZSM-5	372.75	53.9	43.58
Nb(15)ZSM-5	390.18	51.7	41.83
Nb(25)ZSM-5	441.35	45.4	36.72

[a]Calculated from the initial S content of the synthetic fuel.

probably due to overcome of oxide monolayer resulting on steric limitations of the thiophene with the more active sites of the solid.[28]

Effect of temperature and contact time

Table S1 (in the SI section) shows the amount of sulfur removed from the model fuel samples after adsorption for 10 to 360 min, and at temperatures of 301, 333 and 353 K. The results at different temperatures indicate that a greater amount of thiophene was adsorbed at higher temperatures and longer times.

In Figure 3, it can be observed that the adsorbent reaches its saturation time or equilibrium time (t_e) of adsorption at close to 60 min, and the amount of S adsorbed (q_e) by the solid was approximately 46.3 mg g^{-1} for the adsorption curve at 353 K. As the temperature decreased (333 and 301 K), both t_e and q_e also decreased (15 min, 18.3 mg g^{-1} and ≤ 10 min, 6.1 mg g^{-1}, respectively). This shows that the temperature has a relevant effect on the adsorption capacity of these adsorbent materials; in this case, an increase in temperature from 301 to 353 K caused a significant increase (659%) in the amount of adsorbed S, which indicates the occurrence of an endothermic event. Adsorption processes that are endothermic in nature most often are controlled by diffusion (intra-particle diffusion or transport by pore diffusion) or chemisorption.[40]

The deposition of thiophene in the adsorbent led to losses in the apparent surface area of 15.6 and 7% for BET and Langmuir methods, respectively, besides increasing the pore radius of 0.34 nm (Figure 1). An opposite effect was observed for the external surface area of the adsorbent, indicating that the adsorbent had higher amounts of thiophene on the outside of the zeolite (Table 1). Considering that the Nb_2O_5 is on the external surface of the zeolite and that niobium has a significant effect on the adsorption of thiophene, this may indicate that besides reaching the inside of the zeolite, it also interacts with the Nb abroad.

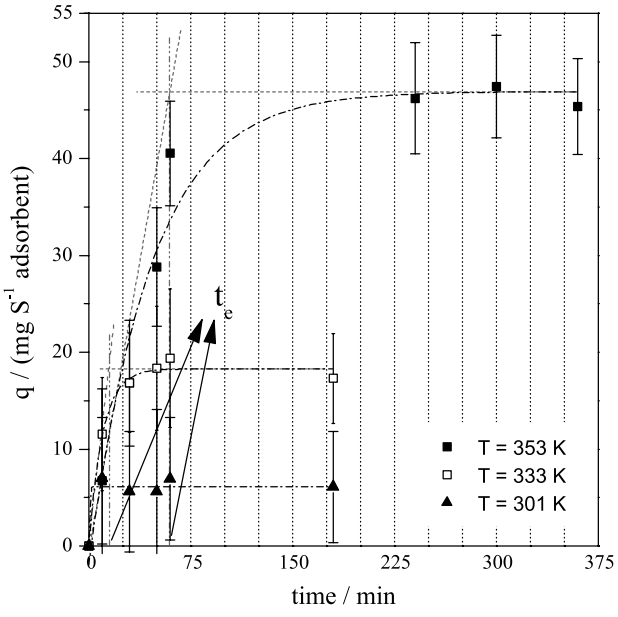

Figure 3. Adsorption of thiophene by the adsorbent Nb(5)ZSM-5 in *iso*-octane as a function of time at different temperatures.

Kinetic study of adsorption

Processes controlled by chemisorption

For analysis of the role of chemisorption in S removal using the adsorbent Nb(5)ZSM-5, the constants K_1, K_2, a and b were obtained from the slopes and intercepts of the graphs that describe PFOE, (Figure 4), PSOE, (Figure 5) and Elovich's (Figure 6) model. The results of the fitting of the models are summarized in Table 3.

The calculated values of q_e for PFOE and PSOE were good approximations of the experimental results. Nevertheless, in terms of the correlation coefficient (r^2), PSOE showed the best match with the experimental data at all temperatures (Table 3). This suggests that the process for removal of thiophene by the adsorbent system Nb(5)ZSM-5 may have as a limiting step a more complex chemisorption phenomenon. Moreover, the increase in the

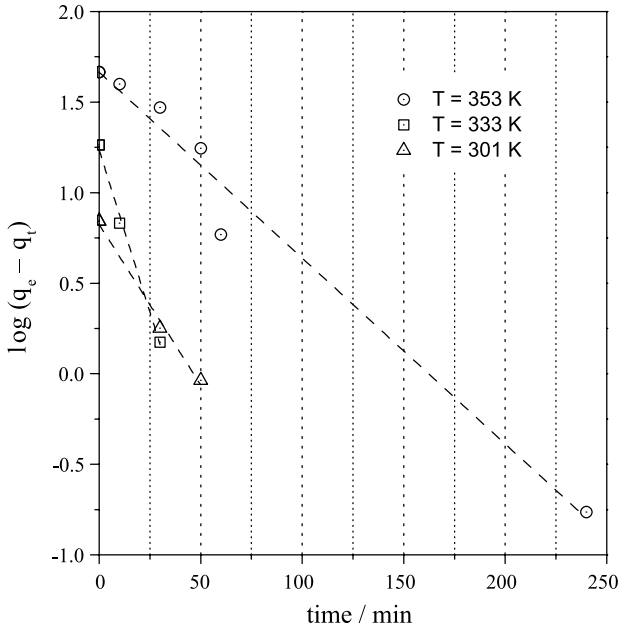

Figure 4. Linear fitting of the data for adsorption of thiophene using the pseudo-first order kinetic model at different temperatures.

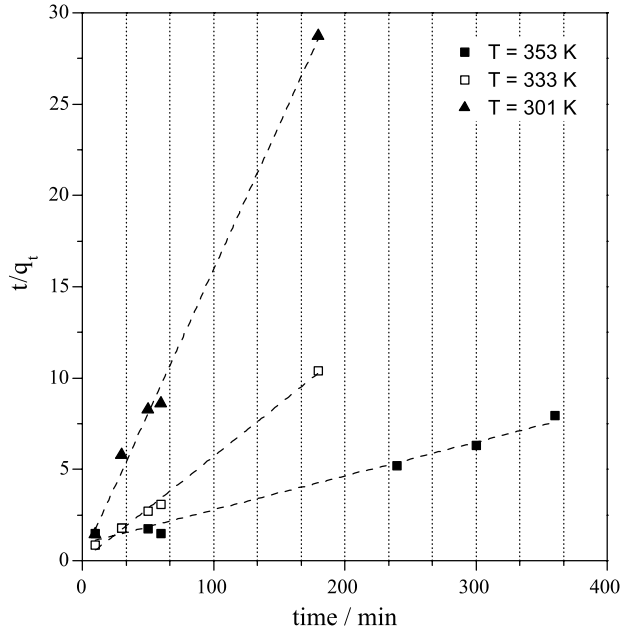

Figure 5. Linear fitting of the data for adsorption of thiophene using the pseudo-second order kinetic model at different temperatures.

adsorbed amount with an increase in temperature confirms that this type of adsorption phenomena is likely.

Processes controlled by diffusion and physisorption

The transport of adsorbate from the liquid phase to the surface of the adsorbent particles can occur at many stages: film or external diffusion, internal diffusion (in pores), surface diffusion and adsorption in the pores of the solid surface. These steps may occur together or separately, or

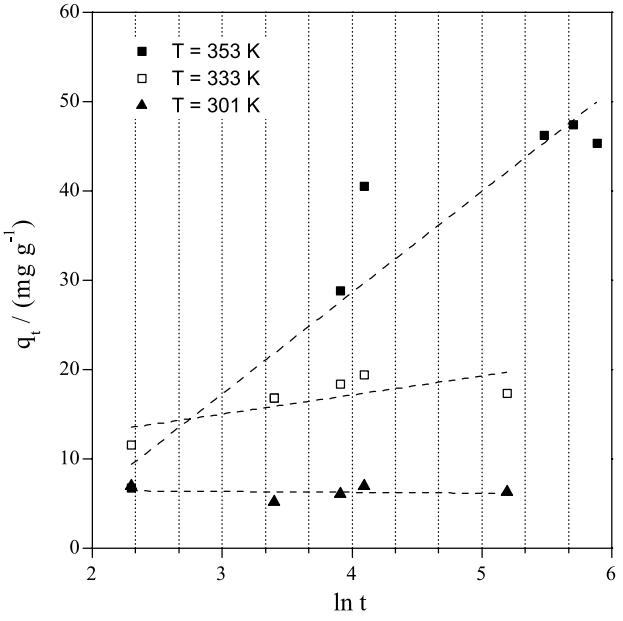

Figure 6. Linear fitting of the data for adsorption of thiophene using the Elovich kinetic model at different temperatures.

Table 3. The kinetic parameters for adsorption of thiophene on Nb(5) HZSM-5 at different temperatures

Kinetic parameter		Temperature / K		
		353	333	301
PFOE	K_1	0.02363	0.08245	0.04086
	$q_{e,cal}$	46.217	17.136	6.692
	r^2	0.9757	0.9949	0.9932
PSOE	K_2	3.738×10^{-4}	0.3785	0.1775
	$q_{e,cal}$	53.881	17.529	6.327
	r^2	0.9836	0.9960	0.9955
Elovich	a	2.5935	122.3455	-2.81×10^{-32}
	b	0.0882	0.4693	−10.5922
	r^2	0.8889	0.5491	0.0180

K_1: rate constant of the pseudo-first order reaction (min^{-1}); K_2: rate constant of the pseudo-second order reaction (g mg^{-1} min^{-1}); r^2: correlation coefficient; a: rate of chemisorption at the initial instant (mg g^{-1} min^{-1}); b: length of the surface coverage for this process (g mg^{-1}); $q_{e,cal}$: amount adsorbed at equilibrium calculated by the kinetic model.

they may not happen at all. To evaluate the magnitude of these factors in regulating the adsorption process, it was evaluated the linear fitting of the data to the intra-particle diffusion and Bangham's models.

From the graphs of q_t *vs.* $t^{1/2}$ for the intra-particle diffusion model (Figure 7a), a multi-linear relationship representing the various stages of diffusion that may be present in the thiophene removal process can be seen.[21,22,41] The values of the intra-particle diffusion constants at different temperatures are listed in Table 4.

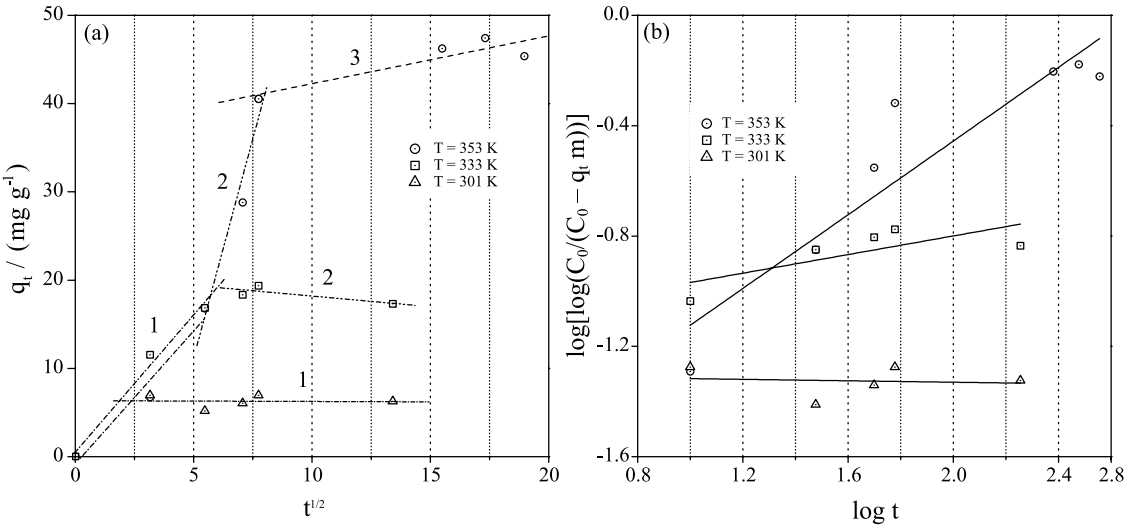

Figure 7. Linear fitting of the data for the adsorption of thiophene using the intra-particle diffusion model (a) and Bangham's model (b) at different temperatures.

Table 4. Kinetic parameters for the intra-particle diffusion of thiophene adsorbed on Nb(5)HZSM-5 at different temperatures

Kinetic parameter	Temperature / K		
	353	333	301
f_1	3.0149	3.1101	–0.0087
C_1	–0.834	0.5117	6.3435
r^2	0.9589	0.9850	0.0020
f_2	9.9271	–0.2416	–
C_2	–38.433	20.6163	–
r^2	0.9509	0.6619	–
f_3	0.5412	–	–
C_3	36.8378	–	–
r^2	0.7893	–	–

f: coefficient of intra-particle diffusion (mg g^{-1} min$^{-0.5}$); C (in mg g^{-1}) is related to the fluid film thickness that surrounds the surface of the solid.

For the isotherm at 353 K, three straight lines were reasonably defined, while for the isotherms at 333 and 301 K, two and one straight lines were observed, respectively. The progressive increase in the multilinearity with increasing temperature can be related to the increased mobility of the adsorbate on the surface and/or inside the adsorbent, resulting in the appearance of new phases with different rates of diffusion. These data may also indicate that high temperature processes involving chemisorption are favored. Regarding the stages of mass transfer and considering that the model for a pseudo-second order reaction fit the experimental data in a reasonable manner, it can be concluded that at high temperatures, the arrival of the adsorbate in the inner regions of the adsorbent by diffusion through the micropores makes the condensation/polymerization of the adsorbate possible, as reported in the work of Yu *et al.*.[42]

To assess whether a diffusion phenomenon in the pores (internal diffusion) is a determinant step in the process, the experimental data were evaluated using the plot log[log(C_0/(C_0 – q_t m))] *vs.* log t (Figure 7b and Table 5).

Table 5. Kinetic parameters for the adsorption of thiophene based on the Bangham's model under different temperatures

Temperature / K	Bangham's model		
	α	K_0	r^2
353	0.6678	0.0338	0.8638
333	0.1687	1.679×10^{-4}	0.5683
301	–0.013	1.144×10^{-4}	0.0113

As observed in Table 5, the experimental results did not fit the model in an acceptable form, indicating that a diffusion mechanism is not the limiting step in the system.[22,25,26,40]

Error analysis

To verify which model best fits the experimental data, seven different error functions were used (Table S2 in the SI section): (*i*) the sum of the square errors (SSE); (*ii*) the sum of the absolute errors (SAE); (*iii*) chi-square (χ^2);[25] (*iv*) the average relative error (ARE);[40] (*v*) the normalized standard deviation (Δq);[43] (*vi*) the hybrid fractional error function (HYBRID); and (*vii*) Marquardt's percent standard deviation (MPSD).[22,40] According to the results obtained, using these methods (Table S3 in the SI section), it was determined that the intra-particle diffusion and PSOE best fit the experimental data for S adsorption at 353 K, with the majority of the results trending to zero (e.g., 0.1688 to χ^2 for intra-particle diffusion). For the

curve at 333 K, the pseudo-first order and intra-particle diffusion models were the best fit. For the adsorption curve at 301 K, Bangham's model showed the best fit to the experimental data (Figure 8).

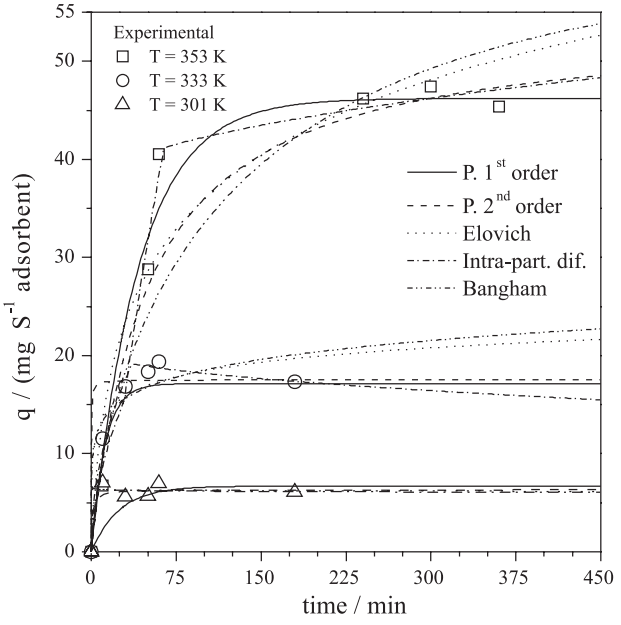

Figure 8. Comparison of the fitted kinetic models and the experimental data for the adsorption of thiophene at different temperatures.

PSOE includes more complex equilibria in the chemisorption process compared to the PFOE. In addition, the Elovich's model considers an exponential increase in the adsorption rate with time. Note that as the temperature changes from 353 to 333 K, there is a change in the model best fitted to the experimental data from pseudo-second to pseudo-first order. As previously mentioned, the increase in adsorption with increasing of temperature can be associated with increased interaction between adsorbate/sites, and thus the change from pseudo-first order to pseudo-second order may indicate a greater variety of interactions between the adsorbate and the adsorbent and thus a more complex equilibrium for the adsorption of thiophene.

The model for intra-particle diffusion applies to the different stages of adsorption, such as external mass transfer followed by intra-particle diffusion in the macro-, meso- and micropores.[21,44] Bangham's model considers the internal diffusion as the rate determining step in the adsorption process based on a logarithmic evolution of the amount adsorbed.[27] As seen in the curves at 333 K and 301 K, the intra-particle diffusion equation gives way to Bangham's equation as the kinetic model best fitted to the experimental data. This change may demonstrate that diffusion and physisorption phenomena are the first steps that occur in the solid.

Finally, it was also observed that the correlation coefficients (r^2), in some cases, are discordant with the results of the error analysis. Although r^2 is an important indicator for assessing a good fit of the model to the data, it does not represent with reliability the performance of the models in comparison with the data, and thus there is a need for error analysis.

Therefore, the solid-liquid system studied here showed by kinetic modeling and error analysis, important contributions of the various types of adsorption observed and these contributions resulted in the highest amount of S adsorbed by the Nb(5)ZSM-5 adsorbent system. Furthermore, under certain conditions (such as high or low temperatures), some types of adsorption and/or mass transfer phenomena prevail.

Estimation of the thermodynamics parameters of adsorption

According to the results obtained from equations 10-12, it was determined that at low temperatures (301 and 333 K), $\Delta G°$ is positive (5.4 and 2.5 kJ mol^{-1}, respectively), while at 353 K, the value becomes negative (−3.5 kJ mol^{-1}), indicating that the adsorption phenomena that appear with an increase in the temperature are spontaneous. The fact that the change in the enthalpy of adsorption ($\Delta H°$) is positive confirms the results obtained in the kinetic study. The positive entropy change indicates that the increase in temperature allows increased degrees of freedom of the solute, which is caused, for example, by increasing the free volume in association with an increased mobility of the adsorbate and a decrease in the retardant forces and interactions in the diffusion process.[24,45-48]

Conclusions

The characterization of the Nb(x)ZSM-5 systems indicated a successful impregnation of Nb_2O_5 in ZSM-5 without changing the structure of the zeolite. The results were also confirmed in the analysis of the physisorption of N_2. The isotherms also exhibited characteristics at high relative pressures that were different from those of microporous structures, which may be associated with the presence of amorphous material or the wide range in particle size, as shown in the SEM analysis. Such a range of particle sizes may also explain the characteristics of the thermodynamic and kinetic adsorption behavior, including the higher adsorption, greater complexity, larger number of steps in the diffusion process, spontaneous processes and entropy increase at higher temperatures.

In the error analysis of the kinetic models, it was observed that the adsorption process occurs by different

processes that occur simultaneously or separately where time and temperature are extremely relevant factors for determining which step(s) will be the rate limiting process(es). Finally, an evaluation of the effect of the Nb_2O_5 content in ZSM-5 on adsorption at different temperatures and reaction times showed that the adsorbent system containing 5 wt.% Nb_2O_5, Nb(5)ZSM-5 at 353 K for 60 min gave the best results, with the amount of adsorbed S equaling 46.3 mg g^{-1}.

Supplementary information

Supplementary information (Figures S1-S2, Tables S1-S3) is available free of charge at http://jbcs.sbq.org.br as PDF file.

Acknowledgements

To CNPq, FAPEAM, UnB-IQ, UFAM-ICE and CBMM (donation of niobium reagents). To the mineralogical technique laboratory of the DGeo-UFAM, analytical laboratory of the CAM-UFAM and LabCat-UnB.

References

1. Hernández-Maldonado, A. J.; Yang, R. T.; *Ind. Eng. Chem. Res.* **2003**, *42*, 123.
2. Speight, J. G.; *The Desulfurization of Heavy Oils and Residua*, 2nd ed.; Marcel Dekker, Inc.: New York, USA, 1999.
3. Babich, I. V.; Moulijn, J. A.; *Fuel* **2003**, *82*, 607.
4. Velu, S.; Ma, X.; Song, C.; *Ind. Eng. Chem. Res.* **2003**, *42*, 5293.
5. Song, C.; *Catal. Today* **2003**, *86*, 211.
6. Pawelec, B.; Navarro, R. M.; Campos-Martin, J. M.; Fierro, J. L. G.; *Catal. Sci. Technol.* **2011**, *1*, 23.
7. Gates, B. C.; *Catalytic Chemistry*; Jonh Wiley & Sons, Inc.: New York, USA, 1992.
8. Shafi, R.; Hutchings, G. J.; *Catal. Today* **2000**, *59*, 423.
9. Valverde Jr., I. M.; Paulino, J. F.; Afonso, J. C.; *Quim. Nova* **2008**, *31*, 680.
10. Malvesti, Á. L.; Mignoni, M. L.; Scherer, R. P.; Penha, F. G.; Pergher, S. B. C.; *Quim. Nova* **2009**, *32*, 1491.
11. Meng, C.; Fang, Y.; Jin, L.; Hu, H.; *Catal. Today* **2010**, *149*, 138.
12. Hernández-Maldonado, A. J.; Yang, R. T.; *Ind. Eng. Chem. Res.* **2003**, *42*, 3103.
13. Yang, R. T.; Hernández-Maldonado, A. J.; Yang, F. H.; *Science* **2003**, *301*, 79.
14. Takahashi, A.; Yang, F. H.; Yang, R. T.; *Ind. Eng. Chem. Res.* **2002**, *41*, 2487.
15. Kox, M. H. F.; Mijovilovich, A.; Sättler, J. J. H. B.; Stavitski, E.; Weckhuysen, B. M.; *ChemCatChem* **2010**, *2*, 564.
16. Jaimes, L.; de Lasa, H.; *Ind. Eng. Chem. Res.* **2009**, *48*, 7505.
17. Ziolek, M.; *Catal. Today* **2003**, *78*, 47.
18. Dąbrowski, A.; *Adv. Colloid Interface Sci.* **2001**, *93*, 135.
19. Campanati, M.; Fornasari, G.; Vaccari, A.; *Catal. Today* **2003**, *77*, 299.
20. Spinelli, V. A.; Laranjeira, M. C. M.; Fávere, V. T.; Kimura, I. Y.; *Polímeros* **2005**, *15*, 218.
21. Carvalho, T. E. M.; Fungaro, D. A.; Izidoro, J. C.; *Quim. Nova* **2010**, *33*, 358.
22. Srivastava, V. C.; Swamy, M. M.; Mall, I. D.; Prasad, B.; Mishra, I. M.; *Colloids Surf., A* **2006**, *272*, 89.
23. Srivastava, V. C.; Mall, I. D.; Mishra, I. M.; *J. Hazard. Mater.* **2006**, *134*, 257.
24. Ranjan, D.; Talat, M.; Hasan, S. H.; *J. Hazard. Mater.* **2009**, *166*, 1050.
25. Naiya, T. K.; Bhattacharya, A. K.; Mandal, S.; Das, S. K.; *J. Hazard. Mater.* **2009**, *163*, 1254.
26. Tütem, E.; Apak, R.; Ünal, Ç. F.; *Water Res.* **1998**, *32*, 2315.
27 Aharoni, C.; Sideman, S.; Hoffer, E.; *J. Chem. Technol. Biotechnol.* **1979**, *29*, 404.
28. Barros, I. C. L.; Braga, V. S.; Pinto, D. S.; de Macedo, J. L.; Rocha Filho, G. N.; Dias, J. A.; Dias, S. C. L.; *Microporous Mesoporous Mater.* **2008**, *109*, 485.
29. Teixeira, V. G.; Coutinho, F. M. B.; Gomes, A. S.; *Quim. Nova* **2001**, *24*, 808.
30. Paulis, M.; Martín, M.; Soria, D. B.; Díaz, A.; Odriozola, J. A.; Montes, M.; *Appl. Catal., A* **1999**, *180*, 411.
31. Neves, C. de F. C.; Schvartzman, M. M. A. M.; *Quim. Nova* **2005**, *28*, 622.
32. Ruthven, D. M.; *Principles of Adsorption and Adsorption Processes*, 1st ed.; John Wiley & Sons, Inc.: New York, USA, 1984.
33. Brunauer, S.; Deming, L. S.; Deming, W. E.; Teller, E.; *J. Am. Chem. Soc.* **1940**, *62*, 1723.
34. Adamson, A. W.; Gast, A. P.; *Physical Chemistry of Surfaces*, 6th ed.; John Wiley & Sons, Inc.: New York, USA, 1997.
35. Šolcová, O.; Matějová, L.; Topka, P.; Musilová, Z.; Schneider, P.; *J. Porous Mater.* **2011**, *18*, 557.
36. Sing, K. S. W.; Everett, D. H.; Haul, R. A. W.; Moscou, L.; Pierotti, R. A.; Rouquérol, J.; Siemieniewska, T.; *Pure Appl. Chem.* **1985**, *57*, 603.
37. Galešić, N.; Brničević, N.; Matković, B.; Herceg, M.; Zelenko, B.; Šljukić, M.; Prelesnik, B.; Herak, R.; *J. Less-Common Met.* **1977**, *51*, 259.
38. Olson, D. H.; Kokotailo, G. T.; Lawton, S. L.; Meier, W. M.; *J. Phys. Chem.* **1981**, *85*, 2238.
39. Bi, J.; Guo, X.; Liu, M.; Wang, X.; *Catal. Today* **2010**, *149*, 143.
40. Mane, V. S.; Mall, I. D.; Srivastava, V. C.; *J. Environ. Manage.* **2007**, *84*, 390.
41. Srivastava, V. C.; Mall, I. D.; Mishra, I. M.; *Colloids Surf., A* **2008**, *312*, 172.

42. Yu, S. Y.; Garcia-Martinez, J.; Li, W.; Meitzner, G. D.; Iglesia, E.; *Phys. Chem. Chem. Phys.* **2002**, *4*, 1241.
43. Wu, F.-C.; Tseng, R.-L.; Juang, R.-S.; *Water Res.* **2001**, *35*, 613.
44. Allen, S. J.; McKay, G.; Khader, K. Y. H.; *Environ. Pollut.* **1989**, *56*, 39.
45. Prasad, R. K.; Srivastava, S. N.; *J. Hazard. Mater.* **2009**, *161*, 1313.
46. Lataye, D. H.; Mishra, I. M.; Mall, I. D.; *Chem Eng. J.* **2009**, *147*, 139.
47. Ho, Y.; *Water Res.* **2003**, *37*, 2323.
48. Ren, Y.; Wei, X.; Zhang, M.; *J. Hazard. Mater.* **2008**, *158*, 14.

Submitted: June 28, 2012
Published online: February 7, 2013